Moist Convective Velocity and Buoyancy Scales

KERRY A. EMANUEL AND MARJA BISTER

Center for Meteorology and Physical Oceanography, Massachusetts Institute of Technology, Cambridge, Massachusetts

(Manuscript received 7 August 1995, in final form 15 April 1996)

ABSTRACT

Velocity, buoyancy, and fractional area scales for moist convection in statistical equilibrium with large-scale forcing are derived using the constraints of global energy and entropy conservation, and subcloud-layer thermodynamic equilibrium. The magnitudes of the velocity and buoyancy in moist convective clouds are shown to depend on cloud microphysical properties and on the vertical distribution, but not the magnitude, of the large-scale forcing. Comparisons of the theoretically derived scales with velocity and buoyancy values observed in a numerical ensemble cloud model and in a one-column radiative-convective model show good agreement.

1. Introduction

Velocity and buoyancy scales for dry convection in statistical equilibrium with an imposed atmospheric cooling and a fixed surface temperature were derived long ago by Prandtl (1925; see also the review by Emanuel et al. 1994). This scaling shows that both the velocity and buoyancy scales increase with the magnitude of the forcing. But, to our knowledge, in the 70 years since Prandtl's work, no theory for moist convective scales has been developed.

The net upward mass flux by convective clouds in statistical equilibrium with large-scale forcing is strongly constrained by the thermodynamic balance between subsidence and radiative cooling in the clear air between clouds. In the absence of large-scale vertical motion, this constraint may be written

$$c_p \frac{T}{\theta}\frac{\partial \theta}{\partial z}\sum_i M_i = -\dot{Q}_{\rm rad}, \qquad (1)$$

where c_p is the heat capacity of air, T and θ are the actual and potential temperatures, M_i represents the ith vertical draft in an ensemble of convective updrafts and downdrafts, and $\dot{Q}_{\rm rad}$ is the radiative heating rate in the clear air. When (1) is coupled with a cloud model that determines the partitioning among up- and downdrafts and the effect of entrainment and detrainment on mass flux, the mass fluxes M_i are determined, though perhaps not uniquely. But while the net upward mass flux is strongly constrained by (1), the partitioning of the mass flux between the fractional area covered by the drafts and their vertical velocity remains undetermined. We can write

$$M_i = \sigma_i (\rho w)_i, \qquad (2)$$

where $(\rho w)_i$ is the mass flux inside the draft and σ_i is the fractional area covered by the draft. Knowledge of M_i does not yield individual scales for σ_i and $(\rho w)_i$.

The lack of knowledge of the correct scaling for velocity and buoyancy in moist convective clouds is a major impediment to progress in understanding the response of convective ensembles to changes in large-scale forcing and in formulating advanced representations of convection in large-scale models. Rennó and Ingersoll (1996) recently proposed an energy method for deducing these scales. Their method predicts that velocity and buoyancy scales increase with the magnitude of the imposed forcing. Robe and Emanuel (1996) performed numerical integrations using a nonhydrostatic cloud model to simulate a field of convective clouds in statistical equilibrium with imposed radiative cooling and surface fluxes. They showed that the buoyancy and velocity scales in the simulated clouds actually remain constant or slightly *decrease* with increasing radiative cooling.

To explain this behavior, we have developed a theory of velocity and buoyancy scales similar to that of Rennó and Ingersoll, but differing in several respects, which we shall discuss.

The theory is presented in section 2 of this report. In section 3 we describe a series of experiments with a one-dimensional radiative–convective equilibrium model and compare the results of these and the numerical experiments of Robe and Emanuel (1996) to the theoretical predictions. These results are discussed and summarized in section 4, which also provides a physical interpretation of the theoretical scales.

Corresponding author address: Dr. Kerry A. Emanuel, Center for Meteorology and Physical Oceanography, Massachusetts Institute of Technology, Room 54-1620, 77 Massachusetts Ave., Cambridge, MA 01239.
E-mail: emanuel@texmex.mit.edu

2. Convective velocity scales from global energy and subcloud-layer thermodynamic balances

Consider a horizontally homogeneous system in a state of radiative–convective equilibrium. The net radiative cooling of the troposphere is balanced by surface sensible and latent heat fluxes, which are redistributed aloft by dry convection in the subcloud layer and by moist convection in the remainder of the troposphere. We define $\bar{Q}_s$ as the net absorption of radiation by the surface:

$$\bar{Q}_s \equiv \mathrm{SW}_{\mathrm{top}} - \Delta\mathrm{SW} - \mathrm{LW}_0, \qquad (3)$$

where $\mathrm{SW}_{\mathrm{top}}$ is the net incoming shortwave radiation at the top of the atmosphere (i.e., the solar flux minus shortwave radiation reflected by the earth, atmosphere, and clouds), $\Delta\mathrm{SW}$ is the reduction of solar radiation owing to absorption by the atmosphere and by clouds, and LW_0 is the net upward longwave flux at the surface.

The mass-integrated radiative heating of the atmosphere is given by

$$\bar{Q}_A = \mathrm{LW}_0 - \mathrm{LW}_{\mathrm{top}} + \Delta\mathrm{SW}, \qquad (4)$$

where $\mathrm{LW}_{\mathrm{top}}$ is the net upward longwave flux at the top of the atmosphere. In general, $\bar{Q}_A$ is negative. Summing (3) and (4) gives

$$\bar{Q}_s + \bar{Q}_A = \mathrm{SW}_{\mathrm{top}} - \mathrm{LW}_{\mathrm{top}} = 0. \qquad (5)$$

In equilibrium there is no net radiative flux at the top of the atmosphere, and thus $\bar{Q}_s = -\bar{Q}_A$.

We shall assume that the absorption and emission of radiation are thermodynamically reversible processes. Then the net change of entropy in the system owing to reversible processes is given by

$$\frac{1}{g}\int\left(\frac{\partial s}{\partial t}\right)_{\mathrm{rev}} dp = \frac{\bar{Q}_s}{T_s} + \frac{\bar{Q}_A}{\bar{T}} = \bar{Q}_A\left(\frac{1}{\bar{T}} - \frac{1}{T_s}\right), \qquad (6)$$

where s is the specific entropy of the system (the entropy of soil or ocean water beneath the surface and the entropy of moist air and cloud in the atmosphere), T_s is the surface temperature, $1/\bar{T}$ is the mean inverse temperature at which radiation is emitted by the atmosphere (including shortwave absorption), the integral is taken over the mass (pressure) of the atmosphere, and g is the acceleration of gravity. Clearly, if $T_s > \bar{T}$, the net production of entropy by absorption and emission of radiation is negative, since $\bar{Q}_s > 0$, $\bar{Q}_A < 0$. In equilibrium, however, the net entropy tendency must be zero since entropy is a state variable:

$$\frac{1}{g}\int\left(\frac{\partial s}{\partial t}\right)_{\mathrm{net}} dp = 0, \qquad (7)$$

implying that there exists an irreversible entropy source,

$$\frac{1}{g}\int\left(\frac{\partial s}{\partial t}\right)_{\mathrm{irr}} dp = \bar{Q}_A\left(\frac{1}{T_s} - \frac{1}{\bar{T}}\right). \qquad (8)$$

Since $\bar{Q}_A < 0$ in the atmosphere and $T_s > \bar{T}$, this will be a positive quantity. This is simply a statement of the second law of thermodynamics.

Many irreversible processes contribute to the entropy source given by (8). These include convective turbulence in the atmospheric and oceanic boundary layers, moist convective turbulence, dissipation owing to falling precipitation, and irreversible sensible and latent heat fluxes from the surface. For the purposes of this scale analysis, we shall neglect all irreversible processes except dissipation of kinetic energy, and shall assume that the majority of dissipation in the system is associated with dry and moist atmospheric convective turbulence. We shall check the validity of this assumption a posteriori (see appendix B). We shall further assume that the convective turbulence is all in the form of dry convection in the subcloud layer and moist convection above the subcloud layer. We shall also neglect dissipation resulting from breaking internal waves.

We next associate irreversible entropy production with dissipation and with buoyancy fluxes. The kinetic energy equation for the atmosphere may be written

$$\frac{\partial}{\partial t}\left(\frac{1}{2}\rho|\mathbf{V}|^2\right) + \nabla\cdot\frac{1}{2}\rho\mathbf{V}|\mathbf{V}|^2 = -\mathbf{V}\cdot\nabla p - \rho g w + \rho\mathbf{F}\cdot\mathbf{V}, \qquad (9)$$

where ρ is the air density, $\mathbf{V}$ the velocity, w the vertical component of velocity, p the pressure, and $\mathbf{F}$ the net frictional force. Integrating over the radiative-convective system in statistical equilibrium gives

$$\int_V [-\mathbf{V}\cdot\nabla p + \rho\mathbf{F}\cdot\mathbf{V}] = 0, \qquad (10)$$

where the notation $\int_V$ indicates an integral over the volume of the system, and the term involving ρw vanishes because there is no net vertical mass flux in equilibrium. This states simply that in equilibrium, pressure work balances dissipation.

We are assuming that frictional dissipation accounts for the entire irreversible entropy source:

$$\int_V T\rho\left(\frac{\partial s}{\partial t}\right)_{\mathrm{irr}} \equiv \bar{T}_{\mathrm{irr}}\int_V \rho\left(\frac{\partial s}{\partial t}\right)_{\mathrm{irr}} = -\int_V \rho\mathbf{F}\cdot\mathbf{V}, \qquad (11)$$

where $\bar{T}_{\mathrm{irr}}$ is the mean temperature at which entropy is produced by irreversible processes. This just states that in a steady system in equilibrium, the irreversible heating equals the dissipation and, from (10), the pressure work, which is the rate at which potential energy is converted to kinetic energy.

In appendix A we show that to a very good approximation, the pressure work integral in (10) may be expressed in terms of the net vertical buoyancy flux:

$$-\int_V \mathbf{V}\cdot\nabla p \approx \int_V MB, \qquad (12)$$

so that (11) and (10) may be combined to give

$$\bar{T}_{\rm irr}\int_V \rho\left(\frac{\partial s}{\partial t}\right)_{\rm irr} \approx \int_V MB, \tag{13}$$

where B is the buoyancy:

$$B \equiv g\frac{\bar{\rho}-\rho}{\rho}.$$

Finally, making use of (8), we get

$$\int_V MB \approx \bar{Q}_A\bar{T}_{\rm irr}\left(\frac{1}{T_s}-\frac{1}{\bar{\bar{T}}}\right). \tag{14}$$

Note that *three* temperatures appear in (14): the mean temperatures at which radiation is absorbed and emitted, and the mean temperature at which kinetic energy is dissipated into heat. The expression (14) departs from Rennó and Ingersoll (1996) in two important respects: First, the integral on the left is the sum over all the turbulent elements of the buoyancy flux, but was approximated by Rennó and Ingersoll as the flux of undilute buoyancy by an undilute updraft; second, the quantity $\bar{T}_{\rm irr}$ appearing in (14) was approximated by T_s in Rennó and Ingersoll (1996). This second approximation produces an error of the order of 10%, and we show presently that the first approximation is only approximately valid in moist convective clouds.

In applying (14) to moist convective velocity scales, it must be recognized that the integral on the left side of (14) includes both moist convective fluxes and dry convective turbulence in the subcloud layer. Symbolically, we write

$$\int_V MB = \int_{\rm sc} MB + \int_{\rm cl} MB, \tag{15}$$

where "sc" and "cl" denote "subcloud layer" and "cloud layer," respectively. We first estimate the first integral on the right side of (15). For this purpose, we suppose that turbulence in a purely convective subcloud layer is generated by radiative cooling of the subcloud layer and by surface fluxes of sensible heat. We also suppose that the turbulent sensible heat flux vanishes at or near the top of the subcloud layer; that is, we neglect the moist convective flux of sensible heat at cloud base. Following through arguments similar to the proceeding, we get

$$\int_{\rm sc} MB \approx \bar{Q}_{A_{\rm sc}}\bar{T}_{\rm irr_{sc}}\left(\frac{1}{T_s}-\frac{1}{\bar{\bar{T}}_{\rm sc}}\right). \tag{16}$$

Thus, the irreversible entropy production in the subcloud layer is approximately balanced by the turbulent buoyancy flux by dry convection. Using this in (15) and (14) gives

$$\int_{\rm cl} MB \approx \bar{Q}_A\bar{T}_{\rm irr}\left(\frac{1}{T_s}-\frac{1}{\bar{\bar{T}}}\right) - \bar{Q}_{A_{\rm sc}}\bar{T}_{\rm irr_{sc}}\left(\frac{1}{T_s}-\frac{1}{\bar{\bar{T}}_{\rm sc}}\right). \tag{17}$$

If the subcloud layer is relatively shallow, the last term in (17) will be relatively small, and in this case

$$\int_{\rm cl} MB \approx \bar{Q}_A\bar{T}_{\rm irr}\left(\frac{1}{T_s}-\frac{1}{\bar{\bar{T}}}\right). \tag{18}$$

This may not be a good approximation, however, when the subcloud layer is deep, as occurs, for example, over dry land.

We now show that in spite of large variations of the moist convective mass flux and buoyancy with height, the integral on the left side of (17) may not be too different from the product of the cloud base mass flux and an undilute buoyancy. Start with a hypothetical undilute updraft of mass flux M_u (by definition, constant with height) and undilute buoyancy B_u. Now consider the effect of turbulent entrainment *alone* on the buoyancy flux:

$$\delta(MB) = M\delta B + B\delta M. \tag{19}$$

In a dry convective plume, buoyancy is linearly mixing, so

$$\frac{\delta B}{B} = -\frac{\delta M}{M}. \tag{20}$$

Thus, in this case, entrainment does not affect the buoyancy flux, and at every altitude $\Sigma_i\, M_iB_i = M_uB_u$.

But in a moist convective plume, buoyancy is *not* linearly mixing and can even change sign owing to entrainment. Moreover, entrainment can actually cause M to change sign locally. In addition to this problem, evaporation and melting of precipitation and condensate loading can cause downdrafts with negative mass flux and negative buoyancy. Thus, in general,

$$\sum_i M_iB_i \neq M_uB_u,$$

where the sum is taken over each individual turbulent element.

To understand how entrainment might affect the buoyancy flux in moist convective clouds, refer to Fig. 1. Here, for reference, the buoyancy and buoyancy flux of a dry plume are shown as a function of the amount of entrained air (Fig. 1a). As more environmental air is added to the plume, the buoyancy decreases but the buoyancy flux remains constant. Figure 1b shows what happens in a moist plume. Owing to evaporation, the buoyancy of the mixture is less than what would result from linearly mixing virtual temperature, and consequently, the buoyancy flux decreases with the amount of entrained air, until all the condensed water has evaporated. Further mixing does not change the buoyancy

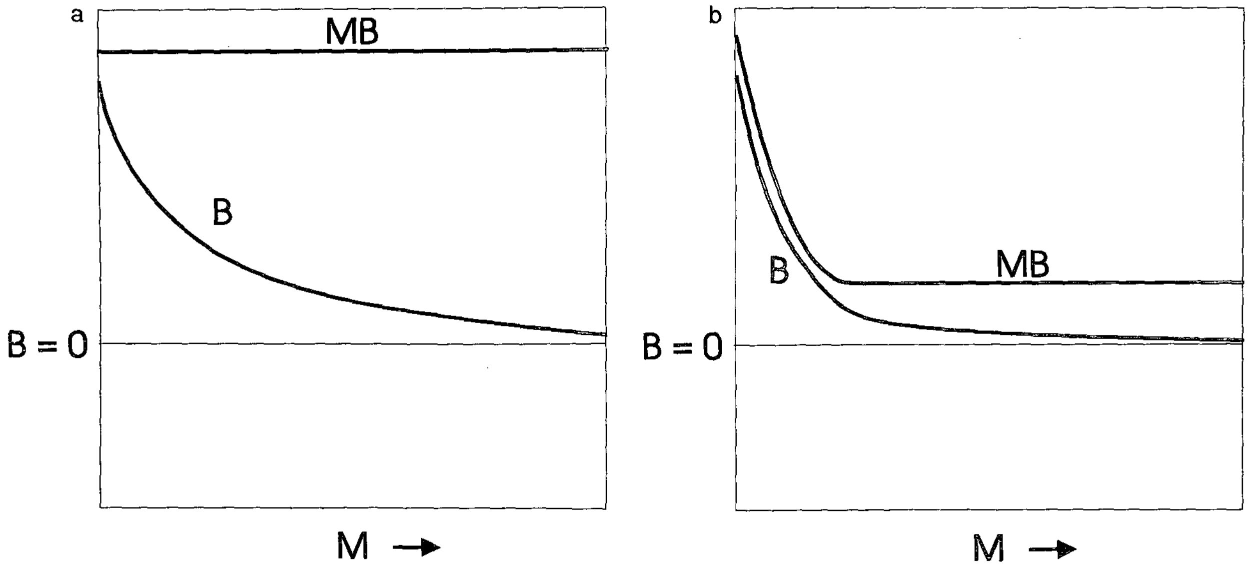

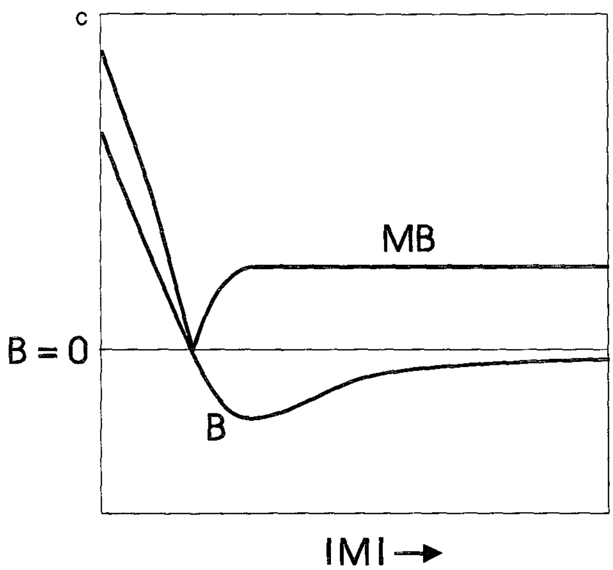

FIG. 1. Effects of entrainment on buoyancy flux. Each graph shows the dependence of buoyancy and buoyancy flux on the amount of entrained mass. (a) Dry convective plume. As the amount of entrained mass increases, the buoyancy becomes more diluted, but the product of buoyancy and mass remains constant. (b) Saturated plume with some cloud water. As more mass is mixed in, condensed water evaporates and both the buoyancy and the buoyancy flux diminish. Once all the condensed water has evaporated, further entrainment does not alter the buoyancy flux, as in (a). In (c) enough cloud water is present so that entrainment eventually leads to buoyancy reversal. Here it is assumed that the sign of the mass flux changes when the buoyancy changes sign. The magnitude of the buoyancy flux, once all the condensed water has evaporated, may be greater than that of the undiluted plume, depending on the cloud and environment thermodynamic properties.

flux. Unless substantial cloud water has been lost by precipitation, the buoyancy can actually change sign (Fig. 1c). If the buoyancy does change sign, its minimum value is reached when just enough environmental air has been entrained to evaporate all of the condensed water (e.g., see Emanuel 1994). Further entrainment diminishes the magnitude of the negative buoyancy but, as before, does not further alter the buoyancy flux.

On this basis, we make a few qualitative deductions about the relationship between the buoyancy flux in actual clouds and the buoyancy flux of undilute air. First, in situations in which much of the condensed water precipitates, entrainment will diminish the buoyancy flux but may not lead to actual buoyancy reversal or, if it does, to small buoyancy reversal. In this case, we may expect that $\Sigma_i M_i B_i < M_u B_u$. In circumstances in which little water precipitates, buoyancy reversal may happen more commonly and penetrative downdrafts may form. As the mass flux in these downdrafts is also negative, it is possible that $\Sigma_i M_i B_i > M_u B_u$ in this case.

Let us take, as a particular case, an example in which $\Sigma_i M_i B_i = M_u B_u$. Then (18) may be written

$$\int_{\rm cl} M_u B_u = M_u \int_{\rm cl} B_u dz = M_u(\text{CAPE}) \approx \bar{Q}_A \bar{T}_{\rm irr}\left(\frac{1}{T_s} - \frac{1}{\bar{T}}\right), \quad (21)$$

where CAPE is the convective available potential energy. The undilute mass flux, M_u, is not a function of height, by conservation of mass, up to the detrainment level. Given an estimate of M_u, which is also the updraft mass flux through cloud base, (21) can be used to predict CAPE. Here we depart substantially from the method used by Rennó and Ingersoll (1996). We close on M_u by using the observation by Raymond (1995) that, in equilibrium, the subcloud layer moist enthalpy budget represents a balance between surface fluxes, radiative cooling, and fluxes out the top of the subcloud layer:

$$\bar{Q}_s + \bar{Q}_{A_{sc}} + M_u(h_m - h_b) = 0, \tag{22}$$

where h_m and h_b represent the average moist static energy of downdraft air and of the subcloud layer, respectively. Using (5), this can be written

$$M_u = \frac{-\bar{Q}_{A_{cl}}}{h_b - h_m}, \tag{23}$$

where $\bar{Q}_{A_{cl}}$ is the radiative heating of the cloud layer. Substituting (23) for M_u into (21) gives

$$\text{CAPE} \approx (h_b - h_m)\left[\frac{\bar{Q}_A \bar{T}_{\text{irr}}\left(\frac{1}{\bar{T}} - \frac{1}{T_s}\right)}{\bar{Q}_{A_{cl}}}\right]. \tag{24}$$

Note that if the integrated radiative cooling of the subcloud layer is a small fraction of the total integrated radiative cooling, we can approximate CAPE by

$$\text{CAPE} \approx (h_b - h_m)\bar{T}_{\text{irr}}\left(\frac{1}{\bar{T}} - \frac{1}{T_s}\right) \equiv \text{CAPE}_p, \tag{25}$$

where CAPE_p is the "predicted" value of CAPE. Also note that we have not really closed the problem, since $h_b - h_m$ must be regarded as part of the solution of the radiative-convective equilibrium problem and cannot be specified as part of the external conditions. As we shall demonstrate, the quantity $h_b - h_m$ can take on different equilibrium values for exactly the same radiative cooling distribution, depending on the values of cloud microphysical parameters, which must be considered at least partially as external parameters (depending, e.g., on cloud condensation nuclei composition and size distribution). Thus, we regard $(h_b - h_m)$ as, to some extent, a surrogate for specification of cloud microphysical parameters. By the aforementioned arguments, we expect the actual CAPE to exceed CAPE_p when entrainment results in little or no buoyancy reversal, and to fall short of CAPE_p when entrainment results in strong buoyancy reversal.

Having derived a moist convective buoyancy scale (25), the vertical velocity scale $\sqrt{\text{CAPE}}$ follows immediately. A fractional area scale then follows from (2):

$$\sigma \approx \frac{-\bar{Q}_A}{\rho(h_b - h_m)^{3/2}\left[\bar{T}_{\text{irr}}\left(\frac{1}{\bar{T}} - \frac{1}{T_s}\right)\right]^{1/2}} \tag{26}$$

We are also now in a position to make an a posteriori estimate of the contribution to irreversible entropy production from sources other than dissipation. Such an estimate is described in appendix B and justifies our neglect of these sources.

In the next section, we test (25) against the results of integrations using a radiative-convective equilibrium model.

3. Experiments with a radiative–convective equilibrium model

We employ the single-column model of Rennó et al. (1994), but replace the calculated radiative cooling with a specified cooling rate. This single-column model uses the convective representation of Emanuel (1991), which is an extension of the buoyancy-sorting algorithm of Raymond and Blyth (1986). The cloud base upward mass flux in the model is calculated by a relaxation toward quasi-equilibrium, and the undilute buoyancy is calculated as part of the solution. The model is integrated with 50-mb vertical resolution.

In the first set of experiments, we attempt to reproduce the experimental conditions used by Robe and Emanuel (1996) by specifying a constant radiative cooling rate from the surface to 175 mb and a constant sea surface temperature of 27.2°C at 1025 mb. The model is integrated until a steady state is achieved.

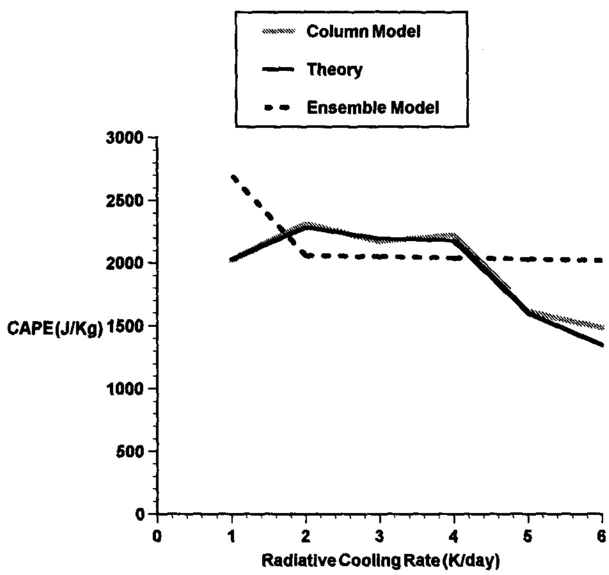

FIG. 2. CAPE as a function of prescribed radiative cooling rate. The dashed curve shows the arithmetic average of reversibly and pseudoadiabatically defined CAPE, averaged over the domain of the ensemble model described by Robe and Emanuel (1996). The hatched line is the CAPE of the equilibrium sounding in a single-column model with parameterized convection. The solid line is the theoretical value of CAPE from Eq. (25), using data from the single-column model.

TABLE 1. Experiments with linearly varying radiative cooling.

Experiment	Cooling profile	CAPE (J kg)$^{-1}$	CAPE$_p$ (J kg)$^{-1}$ [from (25)]
Case I	Increasing with altitude from 1 K day^{-1} to 4 K day^{-1}	3205	3062
Case II	Decreasing with altitude from 4 K day^{-1} to 1 K day^{-1}	680	1259

Nominal (default) values of the microphysical parameters are used in these experiments.

Figure 2 shows the CAPE calculated from the steady-state thermodynamic profiles of the single-column model, as a function of the radiative cooling rate. CAPE is defined for a parcel lifted from the lowest model level. Also shown is the corresponding result from integrating an explicit nonhydrostatic cloud model over a domain large enough to contain many clouds, as reported in this issue by Robe and Emanuel (1996). The curve shown in Fig. 2 represents the arithmetic average of CAPE calculated from reversible and from pseudoadiabatic ascent from the lowest model level. In the single-column model, CAPE is calculated from the actual undilute buoyancy of air lifted from the lowest model level. The single-column model and the full ensemble model produce similar values of CAPE, and variations of CAPE over the range of imposed radiative cooling are of order 10%.

The quantity CAPE$_p$ defined by (25) is calculated from the single-column model data as follows: h_b and h_m are taken to be the moist static energy in the subcloud layer (constant with height in this model) and the moist static energy at 650 mb, respectively. This level is usually near that of the minimum moist static energy. In the cloud layer, we recognize that the mean temperature at which dissipation occurs is a function of the degree of mixing and the draft velocities. For simplicity, we take

$$\bar{T}_{\text{irr}} = \bar{T}, \quad (27)$$

where $\bar{T}$ is the inverse of the vertically averaged inverse temperature, weighted by the radiative cooling rate, as defined previously.

CAPE$_p$ calculated from (25) using the approximations just described is also plotted in Fig. 2. The correspondence with CAPE from the single-column model is striking, considering the approximations used. Correspondence with the results of the ensemble model is not as good, but it must be remembered that the theoretical curve is derived using moist static energies from the single-column model, not from the ensemble model. Even so, the magnitude of CAPE is correctly predicted.

To explore the effects of entrainment, we perform two additional experiments with the goal of encouraging large entrainment but weak or absent buoyancy reversal in one case and strong buoyancy reversal in the other. In the first experiment (case I), the radiative cooling increases linearly with height, from 1 K day^{-1} at the surface to 4 K day^{-1} at 175 mb. This necessitates, through (1), an increasing upward mass flux with height (since the stability decreases with height along a moist adiabat), thus encouraging entrainment into updrafts. The convection is deep, so the precipitation efficiency is high, discouraging buoyancy reversal. In the second experiment (case II), the radiative cooling decreases linearly from 4 K day^{-1} at the surface to 1 K day^{-1} at 175 mb, resulting in a large population of shallow clouds for which buoyancy reversal is prominent. The results of these experiments are summarized in Table 1.

In the case I experiment CAPE is greater than CAPE$_p$ by 143 J kg^{-1}, while in case II CAPE is less than CAPE$_p$ by 579 J kg^{-1}, supporting the arguments presented in section 2. This clearly shows the nonlinearity of buoyancy mixing and the inaccuracy of using CAPE$_p$ to predict CAPE when mixing effects are strong. In percentage terms, the theoretical value of CAPE is especially poor when the cumulus population inated by shallow clouds, which have strong penetrative downdrafts and buoyancy reversal.

We have argued that the appearance of the quantity $h_b - h_m$ in (25) is a consequence of the sensitivity of the equilibrium state to cloud microphysical processes. To test this idea, we performed a number of experiments in which the microphysical parameters in the convective scheme were varied. Figure 3 shows the

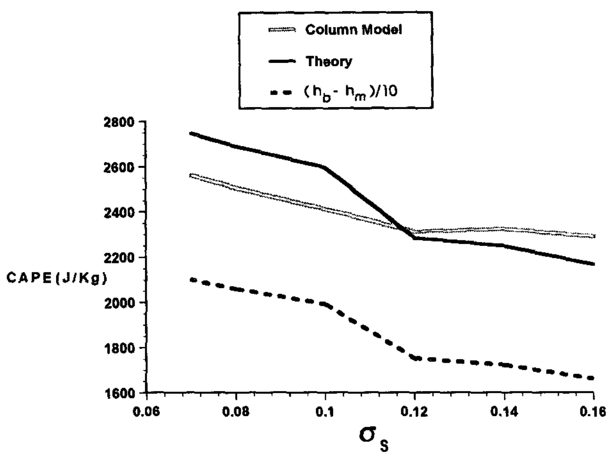

FIG. 3. Actual (hatched) and predicted (solid) values of CAPE from the single-column model, as a function of the prescribed fraction of precipitation falling through unsaturated air, σ_s. The dashed line at the bottom shows 0.1 times the value of $h_b - h_m$.

variation of CAPE and $CAPE_p$ as well as $h_b - h_m$ with the parameter σ_s, which is the fraction of rain assumed to fall outside of cloud in the convective scheme (see Emanuel 1991). The radiative cooling rate is fixed at 2 K day^{-1}. When σ_s is small, little rain evaporates and the equilibrium state is comparatively dry. This should lead to a larger value of $h_b - h_m$ and, thus, through (25), to a larger value of CAPE. This is borne out by the experiments. Clearly, CAPE and $h_b - h_m$ both depend on assumptions about cloud microphysics, not just the large-scale forcing. Drier atmospheres are more unstable, all other things being equal.

4. Discussion

When moist convection and large-scale processes such as radiation and surface fluxes are in a state of statistical equilibrium, the reversible entropy sink owing to absorption and emission of radiation must be balanced by an irreversible source of entropy, if the radiation is absorbed at a higher temperature than it is emitted. In equilibrium, this irreversible entropy source is equal to the integrated dissipation divided by the temperature at which dissipation occurs, neglecting entropy production by mixing and other sources. The dissipation must also equal the rate of conversion of potential to kinetic energy in the system; this in turn is nearly proportional to the integrated buoyancy flux. Thus, we can estimate the vertically integrated buoyancy flux if we know the rate of radiative heating, the mean temperatures at which radiation is absorbed and emitted, and the mean temperature at which dissipation occurs.

Knowledge of the vertically integrated buoyancy flux is not sufficient to determine velocity and buoyancy scales individually. Nor can it be assumed, without some careful reasoning, that the buoyancy flux is equivalent to that carried by an undilute updraft. Indeed, there can be important contributions to energy conversion in convective systems by saturated and unsaturated downdrafts, among other things. We have shown that if downdrafts can be neglected and buoyancy can be assumed to be linearly mixing, then the buoyancy flux by an undilute updraft is the same as that by an entraining plume extending to the same altitude. But in clouds, buoyancy mixing is far from linear, and downdrafts are important. We have shown that entrainment into a saturated updraft reduces the buoyancy flux from that of a nonentraining updraft, while the production of downdrafts of all kinds increases the buoyancy flux. For an undilute updraft, the integrated buoyancy flux is just the cloud base mass flux multiplied by CAPE.

Given a scale for the vertical buoyancy flux, a second relation is needed to find individual scales for buoyancy and mass flux. Here we determine the cloud base mass flux as that required for thermodynamic equilibrium of the subcloud layer. This closure is entirely different from that proposed by Rennó and Ingersoll (1996). When this relation is combined with the energy constraint described above, we arrive at (24). If the subcloud layer is shallow, (24) reduces approximately to (25). We interpret (25) as follows.

As found by Rennó and Ingersoll (1996), the greater the thermodynamic efficiency of the system, as measured by the difference between the temperatures at which radiation is absorbed and emitted, the greater the buoyancy flux must be, and this will in general be associated with higher values of CAPE. But we do not find, as they did, that the buoyancy depends on the *rate* of heat input per se. We regard this discrepancy as owing to the different closure on the fractional area used by Rennó and Ingersoll. Experiments with a full nonhydrostatic model (Robe and Emanuel 1996) and with a single-column radiation–convection model show little dependence of buoyancy on the rate of heat input.

We interpret the predicted value of CAPE given by (25) as follows. If the middle troposphere is relatively humid, then the moist static energy gradient is small. If this is the case, then the static energy deficit of air in downdrafts (including those in clear air outside of clouds) will be small, and to balance the surface entropy flux (which is constrained by the need to balance solar heating of the surface), the downdraft mass flux will have to be relatively large. This implies a relatively large convective updraft mass flux. For the same buoyancy flux, this means that the buoyancy itself must be relatively small.

Aside from comparison with the model results presented here, there is some additional evidence that the buoyancy of convective clouds is correlated with the dryness of the middle troposphere. Ramage (1971) mentions that strong convective events in the Tropics usually occur when the middle troposphere is dry, while heavy but less convective rain is associated with high humidity throughout the troposphere. Radiative-convective equilibrium calculations by Raymond (1994), using a very simple relaxation scheme for convection, also show a strong correlation between cloud buoyancy and middle tropospheric dryness.

5. Summary

We have developed a theory for the buoyancy scales of moist convection in statistical equilibrium with radiation and surface fluxes, based on global energy and entropy conservation and subcloud-layer thermodynamic equilibrium. The theory uses an energy constraint similar to that employed by Rennó and Ingersoll (1996), but constrains the mass fluxes in a very different way. The predictions of our theory differ considerably from those of Rennó and Ingersoll; for example, the buoyancy and velocity scales are independent of the magnitude of the radiative forcing. These predictions compare well with the results of radiative–convective equilibrium calculations using an explicit ensemble cloud model as well as a single-column model. The amount of buoyancy in moist convective clouds depends on the vertical distribution of the forcing, but not on its magnitude, and is also sensitive to cloud microphysical processes. All other things being equal, relatively humid atmospheres will have relatively small buoyancy in clouds. The theory overpredicts CAPE when downdrafts are relatively important (as in nonprecipitating convection) and underpredicts it when there is much entrainment into cloudy precipitating updrafts. Mass conservation demands that for the same vertical mass flux, smaller cloud buoyancy (and thus vertical velocity) be associated with greater fractional areal coverage of updrafts.

We leave to future work the dependence of moist convective buoyancy scales on other forms of large-scale forcing, such as mean ascent. The finding that CAPE can fluctuate depending on the dryness of the middle troposphere implies that strict statistical equilibrium of the kind discussed by Emanuel et al. (1994) may not imply a one-to-one relationship between surface-layer entropy and tropospheric temperature. This might permit non-WISHE (wind-induced surface heat exchange)-type instabilities of the horizontally homogeneous tropical atmosphere. This will be the subject of future work.

APPENDIX A

Near Equivalence of Pressure Work and Buoyancy Flux

The pressure work integral in (10) may be approximated by an integral of the turbulent buoyancy flux, as follows. Divide p into hydrostatic and nonhydrostatic parts,

$$p = \overline{p}_{\rm hy} + p'_{\rm nh}, \tag{A1}$$

where by definition

$$\frac{d\overline{p}_{\rm hy}}{dz} = -\overline{\rho} g \tag{A2}$$

and $\overline{\rho}$ is the time- and horizontal-average density. The pressure work term in (10) can then be expanded:

$$-\int_V \mathbf{V}\cdot\nabla p = -\int_V \mathbf{V}\cdot\nabla\overline{p}_{\rm hy} - \int_V \mathbf{V}\cdot\nabla p'_{\rm nh}. \tag{A3}$$

Using (A2), this becomes

$$\begin{aligned}-\int_V \mathbf{V}\cdot\nabla p &= \int_V w\overline{\rho}g - \int_V \mathbf{V}\cdot\nabla p'_{\rm nh} \\ &= \int_V w\frac{(\overline{\rho}-\rho)}{\rho}\rho g dz + \int_V w\rho g dz - \int_V \mathbf{V}\cdot\nabla p'_{\rm nh}.\end{aligned} \tag{A4}$$

The second integral on the right vanishes because, in equilibrium, there is no net vertical mass flux. Thus the pressure work can be expressed

$$-\int_V \mathbf{V}\cdot\nabla p = \int_V MB - \int_V \mathbf{V}\cdot\nabla p'_{\rm nh}, \tag{A5}$$

where $M \equiv \rho w$ and

$$B \equiv g\frac{\overline{\rho}-\rho}{\rho}$$

is the buoyancy.

Using integration by parts and recognizing that the system is closed, the last term in (A5) can be reexpressed so that (A5) may be written

$$-\int_V \mathbf{V}\cdot\nabla p = \int_V MB + \int_V p'_{\rm nh}\nabla\cdot\mathbf{V}. \tag{A6}$$

The last term on the right of (A6) is difficult to evaluate. It represents a correlation between nonhydrostatic pressure fluctuations and three-dimensional velocity divergence, both of which are usually small. This term vanishes in an anelastic system. For the purposes of deriving appropriate scales, we neglect this contribution and approximate (A6) as

$$-\int_v \mathbf{V}\cdot\nabla p \approx \int_v MB. \tag{A7}$$

APPENDIX B

Estimates of the Magnitude of Neglected Irreversible Entropy Sources

Many processes contribute to irreversible entropy production in moist convective systems, in addition to the mechanical dissipation that was assumed to dominate the other sources. Here we perform an a posteriori check on the magnitude of some of the more important among these other sources. Four of them will be considered: entropy production by evaporation of precipitation in subsaturated air, frictional dissipation associated with falling precipitation, evaporation from the sea surface, and turbulent mixing of air with differing thermodynamic characteristics.

Consider first the entropy production by frictional dissipation associated with falling precipitation. Assuming that all condensed water falls at terminal velocity V_T, the work done by falling precipitation is

$$w_p = \rho_a g l V_T, \tag{B1}$$

where ρ_a is the air density and l is the precipitation mixing ratio. This can be compared to the work done by buoyant convection, $\Sigma_i M_i B_i$, which from the scaling perspective, can be approximated by $M_u B_u$ (see section 2). On the other hand, the mass balance of total water content in statistical equilibrium requires that there be no *net* flux of water through any level:

$$\sum_i M_i(q_{t_i} - q) \approx M_u(q^* - q) = \rho_a l V_T, \tag{B2}$$

where q_{t_i} is the net water content (excluding precipitation) of convective drafts and q^* is the saturation specific humidity. This simply states that in equilibrium, the net flux of water vapor and cloud water by convection is balanced by the net flux of precipitation. If we now define a nondimensional ratio of w_p to the work performed by buoyant convection, we get

$$\frac{w_p}{\sum_i M_i B_i} \approx \frac{w_p}{M_u B_u} \approx \frac{g(q^* - q)}{B_u}, \tag{B3}$$

where we have made use of (B1) and (B2). We now define R_p as the ratio of the vertical integrals of the numerator and denominator of (B3):

$$R_p \equiv \frac{gH_w\overline{(q^* - q)}}{\text{CAPE}}, \qquad \text{(B4)}$$

where H_w is a scale height for water vapor, and $\overline{q^* - q}$ is a mean difference between q^* and q over the depth H_w. For $H_w \approx 3$ km and $\overline{q^* - q} \approx 2$ g kg^{-1}, $R_p \approx 60$ J kg^{-1}/CAPE. For typical values of CAPE predicted by (25), R_p works out to be about 0.05. Thus, from a scaling perspective, neglecting the frictional dissipation of falling precipitation is justified under most circumstances.

Entropy is also produced irreversibly by evaporation under subsaturated conditions. Since air just above the sea surface is subsaturated, evaporation from the ocean will cause an irreversible increase in entropy. The definition of entropy of moist air (Emanuel 1994) is

$$s = (c_{pd} + r_t c_l)\ln T - R_d \ln p_d + \frac{L_v r}{T} - rR_v \ln(\mathcal{H}), \qquad \text{(B5)}$$

where c_{pd} is the heat capacity of dry air, c_l is the heat capacity of liquid water, R_d is the gas constant for dry air, L_v is the latent heat of vaporization, R_v is the gas constant for water vapor, r is the mixing ratio, r_t is the total water mixing ratio, p_d is the partial pressure of dry air, and $\mathcal{H}$ is the relative humidity.

Now consider a system at constant pressure consisting of liquid water and subsaturated air. Some of the liquid water evaporates. Enthalpy, k, is conserved in this process. The definition of enthalpy is (Emanuel 1994)

$$k \equiv (c_{pd} + r_t c_l)T + L_v r. \qquad \text{(B6)}$$

Since enthalpy and total water are both conserved,

$$dk = 0 = (c_{pd} + r_t c_l)dT + d(L_v r). \qquad \text{(B7)}$$

If we differentiate (B5) and make use of (B7), the definition of $r(=(R_d/R_v)(e/p_d))$ and the Clausius–Clapeyron equation, we arrive at

$$ds = -R_v \ln(\mathcal{H})dr. \qquad \text{(B8)}$$

It follows from (B8) that

$$\frac{1}{g}\int\left(\frac{\partial s}{\partial t}\right)_{\text{evap}} dp = -R_v \ln(\mathcal{H})E, \qquad \text{(B9)}$$

where E is the rate of evaporation from the ocean and $\mathcal{H}$ is the near surface relative humidity. On the other hand, the integrated radiative cooling of the atmosphere, $\bar{Q}_A$, is balanced by the surface heat flux, which is of the same order as the latent heat flux:

$$L_v E \sim -\bar{Q}_A. \qquad \text{(B10)}$$

Thus, if we compare the irreversible entropy production by evaporation from the sea to the total irreversible entropy production given by (8) and make use of (B10), we arrive at

$$R_E \equiv \frac{\int\left(\frac{\partial s}{\partial t}\right)_{\text{evap}} dp}{\int\left(\frac{\partial s}{\partial t}\right)_{\text{irr}} dp} \approx \frac{-R_v \ln(\mathcal{H})}{L_v\left(\frac{1}{\bar{T}} - \frac{1}{T_s}\right)}. \qquad \text{(B11)}$$

For $\mathcal{H} = 0.75$, $T_s = 300$ K, and $\bar{T} = 250$ K, $R_E \approx 0.1$. Thus, the irreversible entropy production by evaporation from the sea surface, while not entirely negligible, is about 10% of the total for deep convective equilibrium conditions. There will also be irreversible entropy production owing to sensible heat flux from the sea surface, but this will be small compared to the entropy production by evaporation because, in the first place, the sensible heat flux is usually small compared to the latent flux and, in the second place, the air – sea temperature difference is usually small, in radiative–convective equilibrium.

By extension, we may surmise that the irreversible entropy production by evaporation of precipitation is also small. In the first place, the net evaporation of precipitation must be smaller than the sea surface evaporation, in equilibrium. If the average relative humidity at which precipitation evaporates is not too small, then it follows that (B11) will also serve to compare the magnitude of entropy production by evaporation of precipitation to net entropy production by irreversible processes.

Finally, we consider irreversible entropy production by mixing. We consider the mixing of a cloudy, saturated sample with a clear unsaturated one, but assume that the mixing proceeds slowly enough that the condensed water droplets are always in thermodynamic equilibrium with their environment, unlike the case of evaporating precipitation. Consider two masses of air, m_1 and m_2, that are mixed. Conservation of enthalpy and total water content demand that

$$m_1 \Delta k_1 = -m_2 \Delta k_2 \qquad \text{(B12)}$$

and

$$m_1 \Delta r_{t_1} = -m_2 \Delta r_{t_2}, \qquad \text{(B13)}$$

where k is the enthalpy, given by (B6), and r_t is the total water mixing ratio. On the other hand, *infinitesimal* changes in enthalpy and entropy are related, in this case, by (see, e.g., Emanuel 1994)

$$\delta s = \frac{\delta k}{T} + c_l[\ln(T) - 1]\delta r_t - R_v \ln(\mathcal{H})\delta r. \qquad \text{(B14)}$$

Since $\mathcal{H} = 1$ when any condensed water is present, under the assumption stated above, we can replace δr by δr_t in the last term in (B14), giving

$$\delta s = \frac{\delta k}{T} + c_l[\ln(T) - 1]\delta r_t - R_v \ln(\mathcal{H})\delta r_t. \qquad \text{(B15)}$$

Integrating (B15) over finite changes of enthalpy and entropy gives

$$\Delta s = \frac{\Delta k}{\overline{T}} + \overline{(c_l(\ln T - 1) - R_v \ln \mathcal{H})}\,\Delta r_t, \quad \text{(B16)}$$

where the overbar denotes an average during the change. Using (B16), (B12), and (B13) we can write

$$m_1\Delta s_1 + m_2\Delta s_2 = m_1\Delta k_1\left(\frac{1}{\overline{\overline{T}}_1} - \frac{1}{\overline{\overline{T}}_2}\right) + m_1\Delta r_{t_1}\left(c_l \ln\frac{\overline{T}_1}{\overline{\overline{T}}_2} - R_v \ln\frac{\overline{\mathcal{H}}_1}{\overline{\overline{\mathcal{H}}}_2}\right), \quad \text{(B17)}$$

where $\overline{(\ )}_1$ and $\overline{(\ )}_2$ represent averages experienced by the respective parcels during mixing. As a scaling estimate for Δk_1 we use $h_b - h_m$, the difference between the moist static energy of updrafts and downdrafts, appearing in (23). Similarly, for Δr_t we use a characteristic value of $r_b - r_m$. Using this and (B17), and integrating over the whole system, we obtain an estimate for irreversible entropy production by mixing,

$$\frac{1}{g}\int\left(\frac{\partial s}{\partial t}\right)_{\text{mixing}} dp \sim M_u(h_b - h_m)\left(\frac{1}{\overline{\overline{T}}_1} - \frac{1}{\overline{\overline{T}}_2}\right) + M_u(r_b - r_m)\left(c_l \ln\frac{\overline{T}_1}{\overline{\overline{T}}_2} - R_v \ln\frac{\overline{\mathcal{H}}_1}{\overline{\overline{\mathcal{H}}}_2}\right). \quad \text{(B18)}$$

Using (8) and (23), the ratio of the irreversible entropy production by mixing to the total irreversible entropy production is

$$R_m \equiv \frac{\int\left(\frac{\partial s}{\partial t}\right)_{\text{mixing}} dp}{\int\left(\frac{\partial s}{\partial t}\right)_{\text{irr}} dp} \sim \frac{\frac{1}{\overline{\overline{T}}_1} - \frac{1}{\overline{\overline{T}}_2}}{\frac{1}{\overline{\overline{T}}} - \frac{1}{T_s}} + \frac{(r_b - r_m)\left(c_l \ln\frac{\overline{T}_1}{\overline{\overline{T}}_2} - R_v \ln\frac{\overline{\mathcal{H}}_1}{\overline{\overline{\mathcal{H}}}_2}\right)}{(h_b - h_m)\left(\frac{1}{\overline{\overline{T}}} - \frac{1}{T_s}\right)}. \quad \text{(B19)}$$

Reasonable estimates of the quantities appearing in (B19) yield a value of R_m of about 0.05. Most of this arises from the irreversibility of mixing two parcels with different water contents. The entropy of mixing is comparable in magnitude to the other irreversible processes discussed in this appendix.

While all the processes considered here are at least an order of magnitude less than the total irreversible entropy production, they are strictly additive, so we may expect our approximation that mechanical dissipation accounts for all irreversible entropy production to be off by up to a factor of 2 or so.

REFERENCES

Emanuel, K. A., 1991: A scheme for representing cumulus convection in large-scale models. *J. Atmos. Sci.,* **48,** 2313–2335.

——, 1994: *Atmospheric Convection.* Oxford University Press, 580 pp.

——, J. D. Neelin, and C. S. Bretherton, 1994: On large-scale circulations in convecting atmospheres. *Quart. J. Roy. Meteor. Soc.,* **120,** 1111–1143.

Prandtl, L., 1925: Bericht über Untersuchungen zur ausgebildeten Turbulenz. *Z. Angew. Math. Mech.,* **5,** 136–139.

Ramage, C. S., 1971: *Monsoon Meteorology.* Academic Press, 296 pp.

Raymond, D. J., 1994: Convective processes and tropical atmospheric circulations. *Quart. J. Roy. Meteor. Soc.,* **120,** 1431–1455.

——, 1995: Regulation of moist convection over the west Pacific warm pool. *J. Atmos. Sci.,* **52,** 3945–3959.

——, and A. M. Blyth, 1986: A stochastic model for nonprecipitating cumulus clouds. *J. Atmos. Sci.,* **43,** 2708–2718.

Rennó, N. O., and A. P. Ingersoll, 1996: Natural convection as a heat engine: A theory for CAPE. *J. Atmos. Sci.,* **53,** 572–585.

——, K. A. Emanuel, and P. H. Stone, 1994: Radiative-convective model with an explicit hydrological cycle. Part I: Formulation and sensitivity to model parameters. *J. Geophys. Res.,* **99,** 14 429–14 441.

Robe, F. R., and K. A. Emanuel, 1996: Moist Convective Scaling: Some Inferences from Three-Dimensional Cloud Ensemble Simulations. *J. Atmos. Sci.,* **53,** 3265–3275.